ISSN 1070-3284, Russian Journal of Coordination Chemistry, 2021, Vol. 47, No. 9, pp. 638–645. © Pleiades Publishing, Ltd., 2021.
Russian Text © The Author(s), 2021, published in Koordinatsionnaya Khimiya, 2021, Vol. 47, No. 9, pp. 581–588.

Synthesis, Crystal Structure, and Thermal Properties of Metal-Containing Ionic Liquids with Spiro Cations: $(Spiro)_2MCl_4$ (Spiro = 2,8-Dioxo-5-azoniaspiro[4.5]decane or 2-Oxo-5-azoniaspiro[4.4]nonane, M = Mn, Ni, Co)

M. A. Zakharov[a], *, E. A. Vyatchanina[a], A. S. Ivanov[a], M. A. Bykov[a], E. V. Karpova[a], K. A. Paseshnichenko[a], and L. A. Aslanov[a]

[a] *Moscow State University, Moscow, Russia*

**e-mail: max@struct.chem.msu.ru*

Received January 12, 2021; revised March 25, 2021; accepted March 29, 2021

Abstract—Metal-containing ionic liquids composed of the 2,8-dioxo-5-azoniaspiro[4.5]decane (MorphOx) and 2-oxo-5-azoniaspiro[4.4]nonane (PyrOx) spiro cations and tetrachlorometallate anions MCl_4^{2-} (M = Mn, Ni, Co) were synthesized and studied by X-ray diffraction (CIF file CCDC nos. 2033482 ($MorphOx_2CoCl_4$), 2033483 ($PyrOx_2CoCl_4$), 2033484 ($PyrOx_2MnCl_4$), and 2033485 ($PyrOx_2NiCl_4$)). The compounds $PyrOx_2MCl_4$ are isostructural. The phase transition temperatures of the compounds were determined by differential scanning calorimetry.

Key words: metal-containing ionic liquids, crystal structure, thermal properties

DOI: 10.1134/S1070328421090098

INTRODUCTION

The world energy consumption is increasing from year to year. This demand can be partly met by using renewable energy sources. The intermittent operation of solar batteries and wind power generators requires the design of energy storage devices characterized by high capacity, high energy density, and low cost. These storage devices can be represented by flow batteries, which have been studied rather intensively in recent years [1–3].

A promising design of flow batteries implies the use of ionic liquids (ILs). Ionic liquids are compounds entirely consisting of ions with a melting point below a certain value that is often defined as 100°C; however, in some publications, the maximum melting point of ILs is taken to be 150 or 250°C [4–6]. In the definition of ILs, the indicated maximum temperature specifies an unnecessary restriction [7]. An advantage of ILs over molecular solvents is that polar and ionic compounds are much better solubler in ILs [7], which leads to increasing current density [3]. Ionic liquids have broad electrochemical windows and, owing to zero vapor density, comply with fire safety requirements. The last thirty years, ILs have been studied very intensively. They are used as solvents [8, 9], catalysts [8, 10], single-molecule magnets [11–13], battery electrolytes [14, 15], and for many other applications. In order to find out the trends of variation of their properties following the changes in the structure and composition, it is necessary to know the crystal structure, but for liquids, this is a challenging task [16]. Single crystal X-ray diffraction method has undisputable advantages for determining the atomic structure of compounds; however, it is often of no use for ILs, as they form amorphous (glass-like) states.

One of the trends in the development of low-molecular-weight ILs with high electrochemical stability and moderate viscosity refers to ILs with spiro cations [17–21]. The introduction of an oxygen atom into the cycloalkane chain of the spiro cation decreases the IL melting point and viscosity [22, 23].

Metal-containing ionic liquids have always attracted researchers' attention; various applications of these ILs have been reported [24–26]. The results of studies of metal-containing ILs can be found in our previous publications [27, 28].

In this study, we report the synthesis, crystal structure, and thermal properties of new ionic liquids with spiro cations containing one (2-oxo-5-azoniaspiro[4.4]nonane (PyrOx)) or two oxygen atoms (2,8-dioxo-5-azoniaspiro[4.5]decane (MorphOx)) and halometallate anions MCl_4^{2-} (M = Mn, Ni, Co), particularly, 2,8-dioxo-5-azoniaspiro[4.5]decane tetrachlorocobaltate(II) ($MorphOx_2CoCl_4$) (**I**), 2-oxo-5-azoniaspiro[4.4]nonane tetrachlorocobaltate(II)

($PyrOx_2CoCl_4$) (**II**), 2-oxo-5-azoniaspiro[4.4]-nonane tetrachloronickelate ($PyrOx_2NiCl_4$) (**III**), and 2-oxo-5-azoniaspiro[4.4]nonane tetrachloromanganate(II) ($PyrOx_2MnCl_4$) (**IV**).

The structures of 2-oxo-5-azoniaspiro[4.4]nonane (PyrOx) and 2,8-dioxo-5-azoniaspiro[4.5]decane (MorphOx) spiro cations are depicted below.

PyrOx MorphOx

EXPERIMENTAL

The following chemicals were used: analytical grade $CoCl_2·6H_2O$, $NiCl_2·6H_2O$, and $MnCl_2·6H_2O$; high purity grade P_4O_{10}; and reagent grade $ClCH_2CH_2OH$, pyrrolidine, morpholine, paraformaldehyde, diethyl ether, and CH_2Cl_2.

The chlorides PyrOxCl and MorphOxCl were synthesized according to the following chart: amine (0.4 mol) + paraformaldehyde (0.4 mol) + chloroethanol (0.4 mol) = (150 mL of Et_2O) = $Spiro^+Cl^-$ (amine = pyrrolidine/morpholine, $Spiro^+$ = PyrOx/MorphOx).

Amine was added to a mixture of paraformaldehyde and chloroethanol in diethyl ether. The mixture was stirred at reflux for 3–4 h. Then the reaction mixture was cooled down to room temperature with stirring and, after cooling, it separated into two layers. The upper layer was decanted and the lower layer was mixed with water and filtered. The impurities in the filtrate were extracted three time with dichloromethane. Then the aqueous solution was evaporated to dryness and the residue was dried at 100°C in a vacuum chamber. The yields were 87.5% (PyrOxCl) and 89% (MorphOxCl). T_m(PyrOxCl) = –24°C, T_m(MorphOxCl) = 33°C.

^{1}H NMR (PyrOxCl) (CD_3CN; 293 K; δ, ppm): 2.18 (m, 4H), 3.56 (m, 4H), 3.70 (t, J = 7.7 Hz, 2H), 4.28 (t, J = 7.7 Hz, 2H), 4.74 (s, 2H); ^{1}H NMR (MorphOxCl) (CD_3CN; 293 K; δ, ppm): 3.54 (m, 2H), 3.80 (m, 4H), 3.94 (t, J = 7.5 Hz, 4H), 4.26 (t, J = 7.5 Hz, 2H), 5.00 (s, 2H).

For $C_7H_{14}NOCl$

Anal. calcd., %	C, 51.38	H, 8.62	Cl, 21.66	N, 8.56	O, 9.78
Found, %	C, 50.13	H, 7.78	Cl, 20.72	N, 7.76	O, 13.61

For $C_7H_{14}NO_2Cl$

Anal. calcd., %	C, 46.80	H, 7.86	Cl, 19.74	N, 7.80	O, 17.80
Found, %	C, 45.92	H, 7.04	Cl, 18.82	N, 7.19	O, 21.03

The metal-containing ionic liquids I–IV were synthesized according to the following chart: $2Spiro^+Cl^- + MCl_2·6H_2O = Spiro_2MCl_4 + 6H_2O$ (Spiro = PyrOx/MorphOx; M = Mn, Co, Ni).

$Spiro^+Cl^-$ (2 g; 11.13 mmol of MorphOxCl or 12.22 mmol of PyrOxCl) was placed into a glass weighing bottle with a stopper, and an equimolar amount of $MCl_2·6H_2O$ hydrate (M = Mn, Co, Ni) was added. The mixture was heated to 70–80°C with magnetic stirring for 2–3 h up to complete homogenization. The resulting thick material was placed into a desiccator with P_4O_{10} until crystals precipitated. In the case of compound **IV**, the crystals were obtained after recrystallization from acetonitrile. The products $MorphOx_2CoCl_4$ (**I**) and $PyrOx_2CoCl_4$ (**II**) were air-stable dark blue prismatic crystals. The yields were 94% for **I** and 95% for **II**.

For $(C_7H_{14}NO_2)_2Cl_4Co$ (**I**)

Anal. calcd., %	C, 34.38	H, 5.77	Cl, 28.99	N ,5.73	O, 13.08	Co, 12.05
Found, %	C, 33.80	H, 5.40	Cl, 29.32	N, 5.97	O, 14.00	Co, 11.51

For $(C_7H_{14}NO)_2CoCl_4$ (**II**)

Anal. calcd., %	C, 36.78	H, 6.17	Cl, 31.02	N, 6.13	O, 7.00	Co, 12.89
Found, %	C, 36.11	H, 5.72	Cl, 29.88	N, 5.71	O, 10.05	Co, 12.53

The compound $PyrOx_2NiCl_4$ (**III**) was composed of emerald green prismatic crystals. stable in air. The yield of **III** was 95%.

For $(C_7H_{14}NO)_2NiCl_4$ (**III**)

Anal. calcd., %	C, 36.80	H, 6.18	Cl, 31.04	N, 6.13	Ni, 12.85	O, 7.00
Found, %	C, 36.34	H, 5.80	Cl, 31.22	N, 5.80	Ni, 12.23	O, 8.61

The compound $PyrOx_2MnCl_4$ (**IV**) was composed of lemon-yellow prismatic crystals stable in air. The yield of **IV** was 98%.

For $(C_7H_{14}NO)_2MnCl_4$ (**IV**)

Anal. calcd., %	C, 37.11	H, 6.23	Cl, 31.30	N, 6.18	O, 7.06	Mn, 12.12
Found, %	C, 36.70	H, 5.58	Cl, 31.89	N, 5.71	O, 8.50	Mn, 11.62

Samples of all obtained metal-containing ILs were investigated by differential scanning calorimetry (DSC) on a Netzsch DSC-204 F1 instrument. The measuring system was calibrated according to ISO 11357-1 against parameters of phase transitions of standards (C_6H_{12}, Hg, benzoic acid, Ga, KNO_3, In, Sn, Bi, CsCl, 99.99% purity). The systematic error of the temperature calibration (determined based on In) was 0.1°C.

The samples were tested in standard aluminum cells (V = 56 mm^3, d = 6 mm) crimped with a lid with an orifice (the ratio of the cell bottom area to the orifice area was ~40) in a special purity grade nitrogen flow (40 mL/min) at a heating rate of 5 K/min. Experimental data were treated using the NETZSCH Proteus Analysis package according to ISO/CD 11358.

Single crystal X-ray diffraction study of samples **I–IV** was carried out using a StadiVari Pilatus 100 K sin-

Table 1. Crystallographic data and X-ray experiment and structure refinement details for **I**–**IV**

Parameter	Value			
	I	**II**	**III**	**IV**
Molecular formula	$(C_7H_{14}NO_2)_2Cl_4Co$	$(C_7H_{14}NO)_2Cl_4Co$	$(C_7H_{14}NO)_2Cl_4Ni$	$(C_7H_{14}NO)_2Cl_4Mn$
M	489.13	457.13	456.89	453.13
Radiation (λ, Å)	MoK_α (0.71073)	CuK_α (1.54186)	CuK_α (1.54186)	CuK_α (1.54186)
System	Monoclinic	Monoclinic	Monoclinic	Monoclinic
Space group	$P2_1/c$	$P2_1/c$	$P2_1/c$	$P2_1/c$
a, Å	9.4341(4)	10.4116(3)	10.2935(3)	10.4721(3)
b, Å	16.8689(5)	14.0842(6)	14.0071(4)	14.2173(5)
c, Å	13.2475(7)	13.7810(5)	13.7230(4)	13.8639(4)
β, deg	95.803(4)	90.022(3)	90.412(2)	89.984(2)
V, Å ^{3}	2097.44(16)	2020.83(13)	1978.56(10)	2064.13(11)
Z	4	4	4	4
ρ(calcd.), g/cm^3	1.549	1.502	1.534	1.458
Temperature, K	293(2)	293(2)	293(2)	293(2)
μ, mm^{-1}	1.348	11.597	6.459	10.036
F(000)	1012	948	952	940
Range of θ, deg	2/28.8	4.2/88.8	4.3/73.0	4.2/73.0
Total number of reflections	31252	30252	15128	15802
Number of unique reflections (R_{int})	5350 (0.119)	4614 (0.152)	3846 (0.0367)	3926 (0.059)
Number of reflections with $I > 2\sigma(I)$	2292	1585	3280	2510
Number of refined parameters	227	209	209	209
GOOF on F^2	0.843	0.773	1.031	0.875
R_1 for $I > 2\sigma(I)$	0.0582	0.0560	0.0262	0.0386
wR_2 (for all data)	0.1412	0.1512	0.0691	0.1001
Residual electron density (min/max), e Å^{-3}	–0.675/0.597	–0.499/0.403	–0.387/0.251	–0.243/0.421

gle crystal X-ray diffractometer. The crystal structures were solved by direct methods (SHELX-97 program [29]) and refined by full-matrix least squares method. All atoms except for hydrogens were refined anisotropically (SHELXL program of the SHELX-97 package [29]). The hydrogen atoms were specified geometrically and not refined. The data were treated with the WinGX program [30]. Drawings of the structures were prepared using the Diamond 3.0 program [31]. The crystallographic data and data collection details are summarized in Table 1.

The crystal structure parameters are deposited with the Cambridge Crystallographic Data Centre (CCDC nos. 2033482 (**I**), 2033483 (**II**), 2033484 (**IV**), and 2033485 (**III**)) and can be requested from the authors.

RESULTS AND DISCUSSION

The independent part of the unit cell of **I** consists of two MorhOx cations and one $CoCl_4^{2-}$ anion (Fig. 1). The cation is composed of two rings, mor-

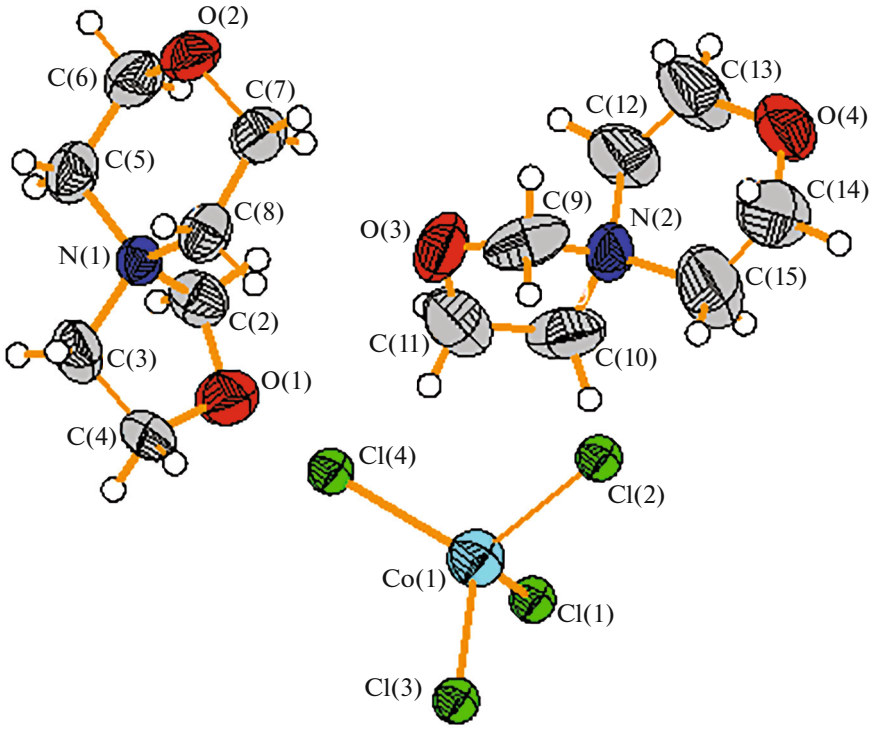

Fig. 1. Fragment of the structure of **I**. Thermal ellipsoids drawn at 50% probability. The hydrogen atom numbering is omitted for clarity.

pholine and oxazolidine rings, sharing a common nitrogen atom. Both cations have the same conformation. The morpholine ring in the cation has a chair conformation, while the oxazolidine ring has a half-chair conformation. Each $CoCl_4^{2-}$ anion is surrounded by nine cations arranged at the corners of a distorted three-capped trigonal prism; four of them contain N(1) atom and five contain N(2) atom. The N(1) cation is surrounded by five anions at the corners of a distorted tetragonal pyramid, while the N(2) cation is surrounded by four anions at the corners of a distorted tetrahedron. The cations form a 3D framework by weak C···O hydrogen bonds (HBs) (with distances from 3.036(7) to 3.538(9) Å), in which the N(2) cations are connected only to N(1) cations, while N(1) cations are also bound to other N(1) cations. The $CoCl_4^{2-}$ anions are located inside the cation framework and contact with the cations via weak C···Cl HBs (3.542(5)–3.821(5) Å) (Fig. 2).

Compounds **II**–**IV** are isostructural. We will consider the structure in relation to compound **II**. The independent part of the unit cell of **II** consists of two PyrOx cations and one $CoCl_4^{2-}$ anion (Fig. 3). The cation is composed of morpholine and oxazolidine rings sharing a common nitrogen atom. The conformations of the rings in both independent cations are similar to the envelope conformation, in which the pyrrolidine ring has carbon atoms in one plane and the nitrogen atom outside this plane. In Fig. 4a, the C(12)–C(13)–C(14)–C(15) carbon atoms of the N(1)-containing cation are located in one plane, while the N(1) atom deviates from this plane, with the C(12)–N(1)–C(15) group being the envelope flap. In the N(2)-containing cation (Fig. 4b), the C(5)–C(6)–C(7)–C(8) atoms are located in one plane, while the C(5)–N(2)–C(8) group is the envelope flap. The oxazolidine ring has a conformation in which the N–C–C–O atoms are in one plane, while the carbon atom between nitrogen and oxygen atoms belongs to the envelope flap. In the N(1)-containing cation, the N(1)–C(10)–C(11)–O(2) atoms are located in one plane, and the C(9) atom is located at the flap apex. In the N(2)-containing cation, the N(2)–C(3)–C(4)–O(1) atoms are located in one plane, while the C(2) atom is at the flap apex. The two cations are conformational diastereomers, as they can be interconverted only upon a conformational change and are not mirror images of each other. For example, if both flaps of the two rings in the N(1) cation (C(9) in the oxazolidine ring and N(1) in the pyrrolidine ring) are bent in the opposite direction, this cation will coincide with the N(2) cation. The same conformations of cations are found in the structure of $PyrOxBF_4$ [23].

The weak C–H···O HBs between the cations combine the cations into layers perpendicular to the *a* axis. The N(1) cation is connected to two N(2) cations via C(12)···O(1) (3.26(1) Å) and C(8)···O(2) (3.382(9) Å)

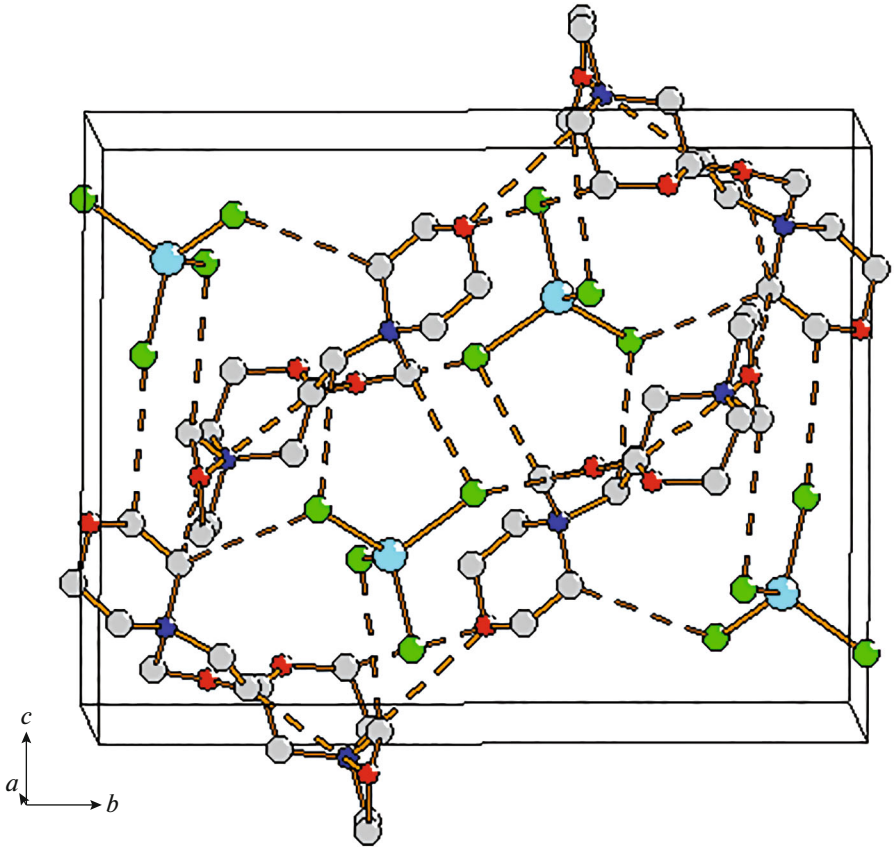

Fig. 2. Hydrogen bonds in the structure of **I**. Hydrogen atoms are omitted for clarity. The dashed lines indicate hydrogen bonds.

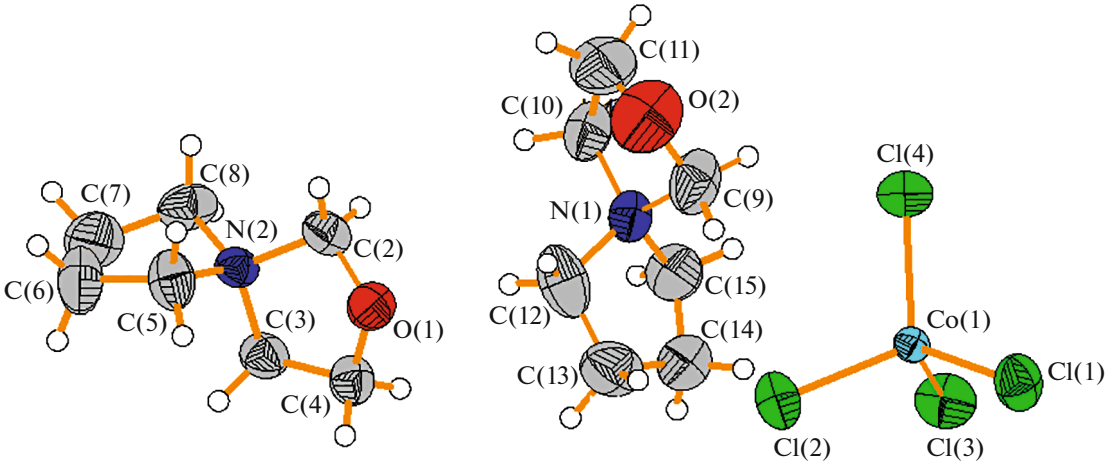

Fig. 3. Fragment of the structure of **II**. The designations of hydrogen atoms are omitted for clarity. The probability of thermal ellipsoids is 50%.

hydrogen bonds, while the N(2) cation is linked to two N(1) cations via C(12)···O(1) (3.26(1) Å) and C(8)···O(2) (3.382(9) Å) hydrogen bonds and to one N(2) cation (which is symmetrically bound to it by an inversion center) via two C(5)···O(1) hydrogen bonds (3.301(8) Å).

Each $CoCl_4^{2-}$ anion is surrounded by eight cations located at the corners of a distorted tetragonal antiprism, four of them containing N(1) atom and the other four containing N(2) atom. Each of the cations is surrounded by four anions at the corners of a distorted tetrahedron. The anions connect the cation lay-

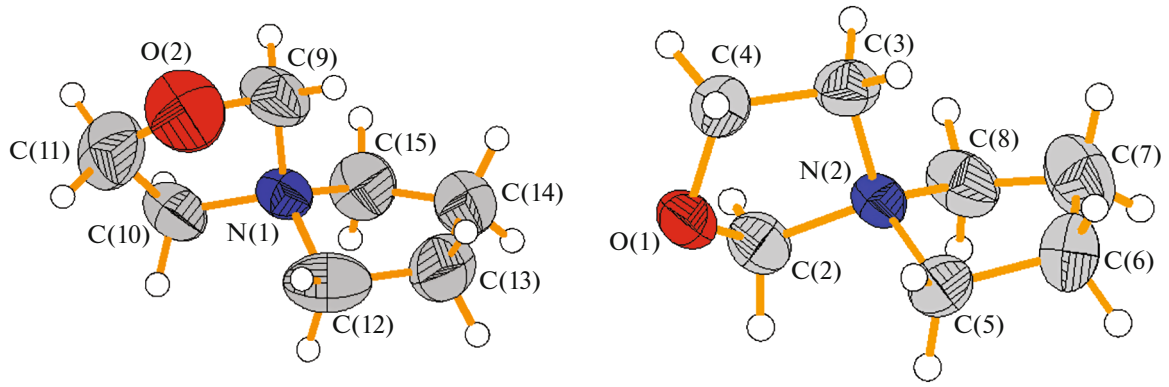

Fig. 4. Conformations of two independent cations: (a) N(1) and (b) N(2) in structures **II**–**IV**.

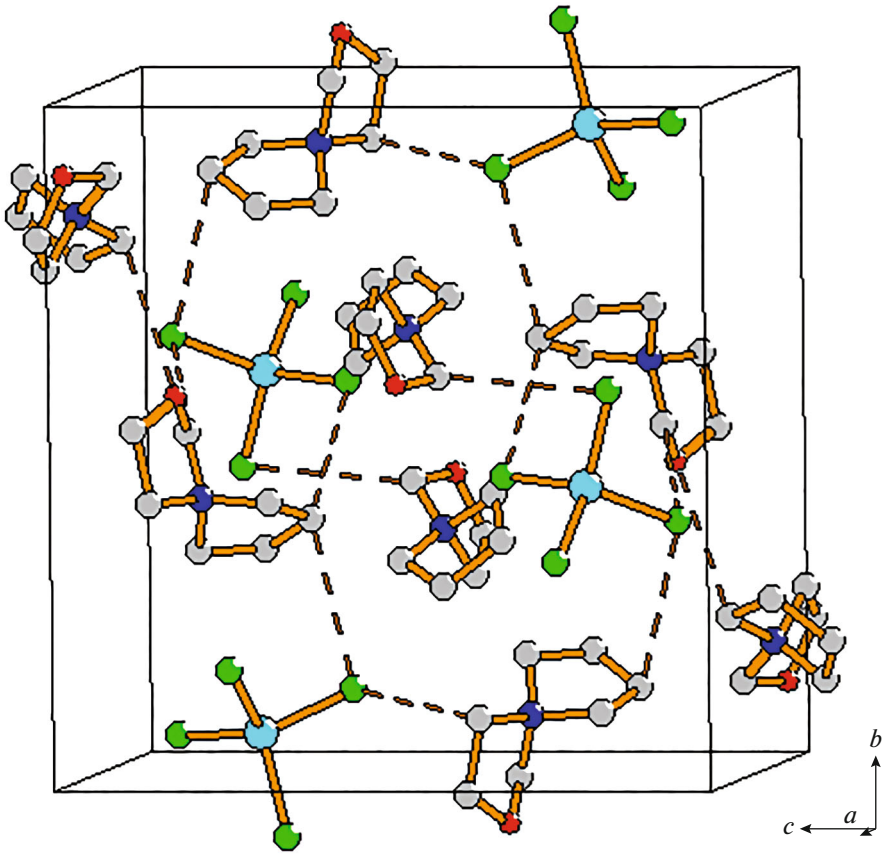

Fig. 5. Hydrogen bonds in the structure of **II**. Hydrogen atoms are omitted for clarity. The dashed lines indicate hydrogen bonds.

ers into a three-dimensional framework via the C–H···Cl hydrogen bonds (C···Cl distances vary from 3.434(8) to 3.688(9) Å) (Fig. 5).

The DSC data for all obtained metal-containing ionic liquids are summarized in Table 2. Sample **IV** has the lowest melting point among these compounds, which is slightly above room temperature. The melting point of **I** is slightly above 100°C; nevertheless, this compound can be classified as an ionic liquid because of its ionic structure and similarity to other ionic liquids considered in this study. In the case of phase **II**, two endothermic phase transitions were found, one of which can correspond to melting (75.2°C), while the other one can be a solid–solid transition (61.1°C). For sample **III**, an exothermic transition was detected, which is apparently attributable to some chemical transformation. To elucidate the nature of transitions

Table 2. DSC data for metal-containing ILs

Sample	T_m, °C	ΔH_m, kJ/mol	$T_{ph.t}$, °C*	$\Delta H_{ph.t}$, kJ/mol
I	118.2	27.964		
II	75.2	2.749	61.1	18.714
III			63.7	128.203
IV	26.8	12.851		

* $T_{ph.t.}$ = phase transition temperature.

in samples of **II** and **III**, additional studies are required.

The melting points of ILs **II**–**IV** are lower than the those of IL **I**. This suggests that the presence of an additional oxygen atom in the IL cation results in a higher melting point. This may be due to the fact that the oxygen atom forms additional hydrogen bonds. Indeed, in the structure of **I**, four oxygen atoms of the cations form seven unique hydrogen bonds, while in the structure of **II**, two oxygen atoms form only four hydrogen bonds. Experimental facts of this type were also observed previously [23]. This assumption is additionally supported by the fact that, according to our data, the melting point of $(MorphOx)_2MnCl_4$ is 39.3°C, which is higher than the melting point of **IV**.

Thus, we synthesized four new metal-containing ionic liquids with the 2,8-dioxo-5-azonia-spiro[4.5]decane (MorphOx) and 2-oxo-5-azonia-spiro[4.4]nonane (PyrOx) spiro cations and MCl_4^{2-} tetrachlorometallate anions (M = Mn, Ni, Co). Their crystal structure was determined by X-ray diffraction; all compounds with the PyrOx cations are isostructural. The phase transition temperatures for the obtained compounds were determined by DSC. On going from the PyrOx cation to the MorphOx, the melting point of the IL increases, which may be attributable to the increase in the number of oxygen atoms in the cation.

ACKNOWLEDGMENTS

The study was carried out using the equipment of the Center for Collective Use of the Moscow State University.

FUNDING

This study was supported by the Russian Foundation for Basic Research (grant no. 19-08-00672a).

CONFLICT OF INTEREST

The authors declare that they have no conflicts of interest.

REFERENCES

1. Soloveichik, G.L., *Chem. Rev.*, 2015, vol. 115, p. 11533.
2. Winsberg, J., Hagemann, T., Janoschka, T., et al., *Angew. Chem., Int. Ed. Engl.*, 2016, vol. 55, p. 2.
3. Noack, J., Roznyatovskaya, N., Herr, T., and Fischer, P., *Angew. Chem., Int. Ed. Engl.*, 2015, vol. 54, p. 9776.
4. Aslanov, L.A., Zakharov, M.A., and Abramycheva, N.L., *Ionnye zhidkosti v ryadu rastvoritelei* (Ionic Liquids in the Series of Solvents), Moscow: Moscow State University, 2015.
5. Zlotin, S.G. and Makhova N.N., *Usp. Khim.*, 2010, vol. 79, no. 7, p. 603.
6. Marcus, Y., *Ionic Liquid Properties. From Molten Salts to RTILs*, Springer, 2016.
7. MacFarlane, D.R., Kar, M., and Pringle, J.M., *Fundamentals of Ionic Liquids. From Chemistry to Applications*, Wiley-VCH, 2017.
8. Vekariya, R.L., *J. Mol. Liq.*, 2017, vol. 227, p. 44.
9. Greaves, T.L. and Drummond, C.J., *Chem. Rev.*, 2015, vol. 115, p. 11379.
10. Dai, C., Zhang, J., Huang, C., and Lei, Z., *Chem. Rev.*, 2017, vol. 117, p. 6929.
11. Yoshida, Y., Tanaka, H., Saito, G., et al., *Inorg. Chem.*, 2009, vol. 48, p. 9989.
12. Yoshida, Y. and Saito, G., *J. Mater. Chem.*, 2006, vol. 16, p. 1254.
13. Hayashi, S. and Hamaguchi, H.O., *Chem. Lett.*, 2004, vol. 33, p. 1590.
14. Hapiot, P. and Lagrost, C., *Chem. Rev.*, 2008, vol. 108, p. 2238.
15. Watanabe, M., Thomas, M.L., Zhang, S., et al., *Chem. Rev.*, 2017, vol. 117, p. 7190.
16. Hayes, R., Warr, G.G., and Atkin, R., *Chem. Rev.*, 2015, vol. 115, p. 6357.
17. Ue, M., Ida, K., and Mori, S., *J. Electrochem. Soc.*, 1994, vol. 141, p. 2989.

18. Clough, M.T., Geyer, K., Hunt, P.A., et al., *Phys. Chem. Chem. Phys.*, 2016, vol. 18, p. 3339.
19. Yu, C., Iwama, E., Ueda, T., et al., *J. Phys. Chem.*, 2020, vol. 124, p. 12230.
20. Nguyen, H.V.T., Lee, S., Kwak, K., and Lee, K.-K., *Electrochim. Acta*, 2019, vol. 321, p. 134649.
21. Xu, L., Gao, J.-X., Chen, X.-G., et al., *Dalton Trans.*, 2018, vol. 47, p. 16995.
22. Devarajan, T., Higashiya, S., Dangler, C., et al., *Electrochem. Commun.*, 2009, vol. 11, p. 680.
23. Higashiya, S., Filatov, A.S., Wells, C.C., et al., *J. Mol. Struct.*, 2010, vol. 984, p. 300.
24. Estager, J., Holbrey, J.D., and Swadzba-Kwasny, M., *Chem. Soc. Rev.*, 2014, vol. 43, p. 847.
25. Brown, L.C., Hogg, J.M., and Swadzba-Kwasny, M., *Top. Curr. Chem.*, 2017, vol. 375, p. 1.
26. Meyer, C., Werner, S., Haumann, M., and Wasserscheid, P., *Ionic Liquids Completely UnCOILed: Critical Expert Overviews*, Wiley, 2015, p. 107.
27. Zakharov, M.A., Filatova, Y.V., Bykov, M.A., et al., *Russ. J. Coord. Chem.*, 2020, vol. 46, no. 4, p. 268. https://doi.org/10.1134/S1070328420040077
28. Zakharov, M.A., Fetisov, G.V., Veligzhanin, A.A., et al., *Dalton Trans.*, 2015, vol. 44, p. 18576.
29. Sheldrick, G.M., *Acta Crystallogr., Sect. A: Found. Crystallogr.*, 2008, vol. 64, p. 112.
30. Farrugia, L.J., *J. Appl. Crystallogr.*, 1999, vol. 32, p. 837.
31. *Diamond. Crystal and Molecular Structure Visualization*, Bonn: Crystal Impact, 2014.

Translated by Z. Svitanko